PHYSICAL REVIEW E **73**, 010502(R) (2006)

Hydrodynamic field around a Brownian particle

P. Keblinski[1,*] and J. Thomin[2]
[1]*Materials Science and Engineering Department, Rensselaer Polytechnic Institute, Troy, New York 12180-3590, USA*
[2]*Chemical and Biological Engineering Department, Rensselaer Polytechnic Institute, Troy, New York 12180-3590, USA*
(Received 24 August 2005; published 27 January 2006)

We use molecular dynamics simulations of a solid Brownian particle in an explicit solvent to analyze the velocity field generated by a stochastic motion of a particle. The simulation data demonstrate that the amplitude of the velocity field around a Brownian particle decays much faster than the velocity field around a particle moving with a constant velocity. However, the time-integrated response of the velocity field around a Brownian particle has exactly the same distance dependence as the velocity field around a particle moving with a constant velocity. This finding elucidates the validity of an assumption used in theoretical descriptions of Brownian particles dynamics in confined geometries and in colloids; namely, that viscous drag forces can be computed as if the particles move with constant velocities.

DOI: 10.1103/PhysRevE.73.010502 PACS number(s): 83.10.Mj, 83.80.Hj

A spherical particle moving with a constant velocity in a stationary fluid generates a long-range velocity field $V(\mathbf{r})$ that decays as the inverse of the distance from the sphere center, $V(\mathbf{r}) \sim 1/r$ [1]. This long-range velocity field modifies the drag force on the particle in narrow channels due to boundary conditions imposed by the walls [2]. The same velocity field leads to long-range hydrodynamic interactions in colloids [3]. In a standard and accepted approach to the problem of diffusing Brownian particles in confined geometries or in suspensions, the forces acting on particles are calculated as if particles' velocities are constant [2]. This treatment yields results that are in excellent agreement with experimental data [4].

The problem of the velocity field around Brownian particles is also relevant to a recent hypothesis that unusually high enhancements of thermal conductivity observed in fluid suspensions of nanosized particles (nanofluids) are due to hydrodynamic effects of the Brownian motion of nanoparticles [5–7]. The argument here is that, due to long-range velocity fields, the large volumes of fluid are dragged by nanoparticles and carry a substantial amount of heat.

It is, however, puzzling how a Brownian particle that rapidly changes the direction of its motion is capable of generating a long-range velocity field quantitatively the same as that present around a particle moving with a constant velocity. In particular, during a short relaxation time, characteristic of the Brownian motion, a hydrodynamic signal propagates only over a distance comparable with the particle size, which does not appear sufficient to establish a velocity field with a substantial range.

Related conceptual difficulty was recognized in the context of the calculation of diffusivity of Brownian particles [8]. In this case the Stokes-Einstein formalism assumes that a drag coefficient is computed as if the particle velocity is a constant. This assumption allows us to write down a Langevin dynamics equation of motion:

$$m\frac{dv}{dt} = -6\pi\eta R v + F(t), \tag{1}$$

describing the motion of a particle with radius R and mass m that is moving in a fluid of viscosity η under the influence of the viscous drag force and a stochastic force, $F(t)$. The drag force $-6\pi\eta R v$ is only a function of an instantaneous velocity and does not depend on the particle motion history. Despite these simplifications, this approach captures essential features of the Brownian motion and leads to the quantitatively correct Stokes-Einstein formula for particle diffusivity, $D = k_B T/6\pi\eta R$. In fact, it was rigorously demonstrated that while the exact treatment of the particle motion requires incorporation of the memory effects in the Langevin equation, the diffusion constant is only dependent on the time-integrated viscous drag coefficient, which is exactly the same as the viscous drag coefficient for a stationary motion [8].

In our work, rather than focusing on the particle motion, we will analyze the velocity field around a Brownian particle. First, we present an estimate of the range of the hydrodynamic field around a Brownian particle. An analysis of Eq. (1) leads to a characteristic Brownian relaxation time,

$$\tau_B = m/6\pi\eta R, \tag{2}$$

over which the particle moves in a deterministic manner. During this time a hydrodynamic signal propagating by a viscous shear travels by a distance, λ:

$$\lambda = \sqrt{\nu\tau_B} = \frac{\sqrt{2}R}{3}\sqrt{\frac{\rho_P}{\rho_F}}, \tag{3}$$

where $\nu = \eta/\rho_F$ is the kinematic viscosity, and ρ_P and ρ_F are densities of the particle and the fluid, respectively. Also, in the derivation of Eq. (3) we used $m = 4\pi\rho_P R^3/3$. For particles with density matching the density of the fluid, λ is about half of the particle radius, and even for dense solid particles λ is of the order of the particle diameter. This estimate shows that the range of the velocity field associated with the dominant

*Electronic address: keblip@rpi.edu

frequency component of the Brownian motion is of the order of a particle size, which is indeed much shorter than a very long-range field around a particle moving with a constant velocity.

To elucidate the apparent contradiction between the estimate presented above and well-known long-range effects affecting the Brownian motion we performed equilibrium molecular dynamics simulations of a single nanoparticle embedded in a simple molecular fluid. The interactions between fluid atoms are described by the standard 6–12 Lennard-Jones (LJ) potential, with a cutoff distance $R_C = 2^{1/6}\sigma$, where σ is the unit of length. The selected cutoff distance corresponds to the minimum of the LJ potential. Consequently, all fluid interatomic interactions are purely repulsive. The solid particle is formed by carving out a sphere out of a fcc lattice of atoms. These atoms, in addition to the repulsive LJ interaction, are connected with the nearest neighbors by attractive springs (FENE potential [9]). The selected number of atoms in a particle is 296, leading to a radius, $R \approx 4\sigma$. To mimic solid particles, the masses of atoms forming nanoparticles are 3 times larger than the mass of the fluid atom, resulting in a particle density about 4.5 times larger than the fluid density. The particle is dissolved in 50 000 and 90 000 fluid atoms at a reduced fluid density of 0.81. The corresponding cubic simulation box sizes are about 40 and 48σ, respectively, i.e., 10 and 12 times the particle radius. The molecular dynamics (MD) simulations are performed at constant volume and temperature, $T = 1.0\varepsilon/k_B$, where ε is the LJ energy unit. A MD time step of $0.005\tau_{MD}(\tau_{MD} = \sqrt{\varepsilon/m\sigma^2})$ and the velocity-Verlet integration algorithm are used in all simulations [10]. Each simulation run consists of 200 000 MD step equilibration and 1 000 000 MD step data production.

During the simulation we collect the x, y, and z components of the particle velocity, as well as the velocities of concentric fluid shells of thickness 1σ. From such obtained data we calculate the nanoparticle velocity autocorrelation function, $\langle \mathbf{V}_{NP}(t)\mathbf{V}_{NP}(0)\rangle$, where the triangular brackets denote the time average. To quantify the relationship between the nanoparticle motion and the velocity field around the particle we monitor the cross velocity correlation functions between the nanoparticle and concentric fluid shells, $\langle \mathbf{V}^r_{shell}(t)\mathbf{V}_{NP}(0)\rangle$, where r indicates the distance of the shell from the particle center, with $r = 1.1$ R corresponding to the 1σ thick fluid layer adjacent to the particle.

In Fig. 1 we show the particle velocity autocorrelation function (VAF), of the nanoparticle for the two system sizes studied. The nanoparticle VAF value at $t = 0$ corresponds to the square of the average thermal velocity, while the inverse of the VAF rate of decay corresponds to the Brownian relaxation time, τ_B. The τ_B obtained from the exponential fit to the VAF for 50 000 and 90 000 atom structures equal to $7.3\tau_{MD}$ and $9.9\tau_{MD}$, respectively, indicating that the particle in the larger simulation box is more mobile. Accordingly, the diffusion constants obtained from the integral of the VAF for the 50 000 and 90 000 atom structures are 5.9 and 7.2 $\times 10^{-3}\sigma^2/\tau_{MD}$, respectively, and show a significant size effect associated with the long-range nature of hydrodynamic forces.

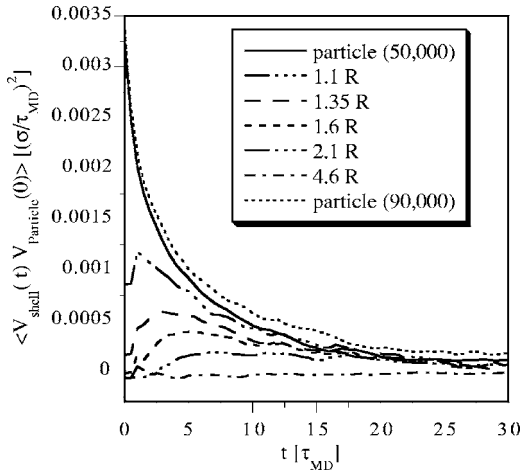

FIG. 1. The solid black line is the velocity autocorrelation function (VAF) of the particle in the 50 000 fluid atom structure, while the dotted black line shows VAF for the particle in the 90 000 fluid atom structure. The other data show cross correlations between the velocity of the particle in the 50 000 fluid atom structure and velocities of concentric fluid shells of thickness 1σ, located at various distances from the particle center (distance 1.1 R corresponds to the fluid layer immediately adjacent to the particle surface).

In Fig. 1 we also show particle-fluid cross velocity correlations. These correlations show that the instantaneous velocity field around a Brownian particle is very different from the one around a particle exhibiting a constant velocity motion. The fluid layer immediately adjacent to the particle is strongly correlated with the particle motion. This is characteristic of the nonslip boundary condition. However, with increasing distance from the fluid, the response is delayed. In fact, at distances larger than about 2 R, the peak response time is proportional to r^2 (see Fig. 2), consistent with the diffusive viscous shear signal propagation in the Newtonian fluid flow [1].

The magnitude of the peak response of the velocity cor-

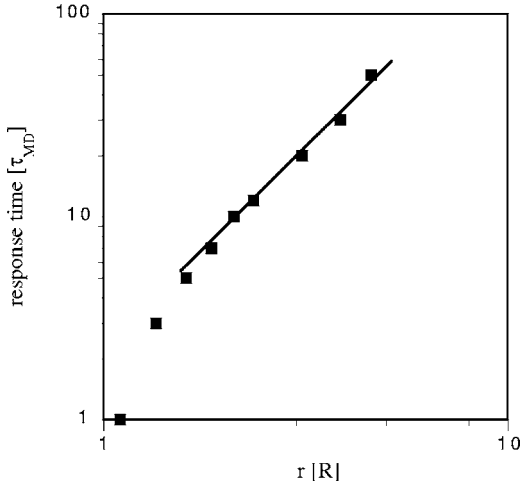

FIG. 2. A time corresponding to the peak position of the fluid-particle cross-correlation functions from Fig. 1 as a function of the distance from the particle center (in units of particle radius) on a log-log plot. The solid line indicates a slope of 2.

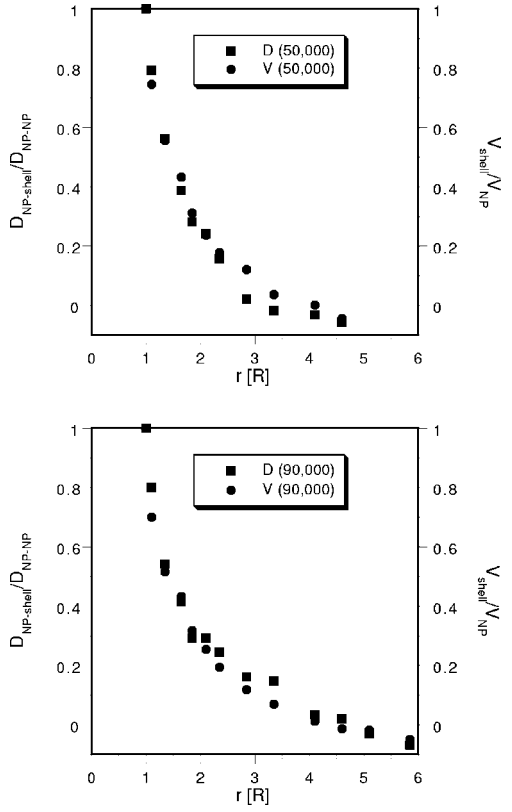

FIG. 3. Squares: Time integrals of the fluid-particle cross-correlation functions normalized by the time integral of the particle VAF as a function of the distance from the particle center for 50 000 and 90 000 fluid atom structures. Circles: Velocity of the fluid shells normalized by the particle velocity in the constant velocity simulation.

relation function decays rapidly with increasing distance from the nanoparticle. For the shell located at $r=2.6$ R from the center of the particle, the peak value of the velocity field correlated with the particle motion retains only 5% of the $\langle \mathbf{V}_{NP}(0)\mathbf{V}_{NP}(0)\rangle$ value. Furthermore $\langle \mathbf{V}_{shell}^{2.6\ \mathrm{R}}(t)\mathbf{V}_{NP}(0)\rangle$ is very smooth and does not reflect the sharp time decay of the nanoparticle VAF. This demonstrates that as the distance from the nanoparticle increases, the surrounding fluid responds only to the "average" motion of the particle, and not to the instantaneous velocity.

While the peak value of the correlated velocity field decays rapidly with the distance from the particle, the time-integrated correlations are much more persistent as demonstrated in Fig. 3 by the integral of the $\langle \mathbf{V}_{shell}^{r}(t)\mathbf{V}_{NP}(0)\rangle$ normalized by $\int\langle \mathbf{V}_{NP}(t)\mathbf{V}_{NP}(0)\rangle$ plotted as a function of r. This is a result of the increasing width of the peak that to a large extent compensates for the decreasing peak value.

To provide a reference for the spatial range of the time-integrated correlations we simulated a Brownian particle subjected to a constant force of $5\varepsilon/\sigma$ acting along the x direction. To conserve momentum (as is the case for our Brownian particle simulations), an equal and opposite force was applied uniformly to the fluid. This external force leads to particle drift with an average velocity comparable with the r.m.s. of the thermal velocity.

Quite remarkably, as demonstrated in Fig. 3, we find that

$$\frac{\int \langle \mathbf{V}_{shell}^{r}(t)\mathbf{V}_{NP}(0)\rangle dt}{\int \langle \mathbf{V}_{NP}(t)\mathbf{V}_{NP}(0)\rangle dt}(Brownian) = \frac{\mathbf{V}_{shell}^{r}}{\mathbf{V}_{NP}}(stationary), \tag{4}$$

i.e., that the integrated particle-fluid velocity correlations normalized by the integrated particle VAF for a particle exhibiting Brownian motion are quantitatively the same as the shell velocities normalized by the particle velocity for a particle exhibiting a stationary motion. Our empirical observation given by Eq. (4), demonstrates that, in practice, the velocity field around a Brownian particle can be treated as if the particle moves with a constant velocity.

From the steady velocity simulations we extracted viscous drag coefficients [see Eq. (1)] $6\pi\eta R=181$ and $156\sqrt{\varepsilon^3 m}/\sigma^3$, for 50 000 and 90 000 atom structures, respectively, again showing large size effects. In fact, due to periodic boundary conditions applied in our simulations, our steady velocity simulations are equivalent to the problem of a fluid flow past a periodic cubic array of spheres separated by a distance equal to the simulation box size. The analytical solution of this problem predicts about 5% relative difference between the viscous drag coefficients exhibited by spheres in the large and small simulation cells, respectively [11]. The actual simulations results show significantly larger 15% relative difference. This discrepancy between the theoretical prediction and simulations results might be associated with the fact that the nonslip boundary condition at the particle-fluid interface is not rigorously satisfied. In fact, a close examination of the velocity profiles for larger and smaller simulation cells indicates a larger velocity slip at the fluid-particle interface for the larger system (Fig. 3).

The values of the drag coefficient calculated from the steady velocity simulations allow us to calculate the particle diffusivity from the Stokes-Einstein formula yielding D of 5.5×10^{-3} and $6.4\times10^{-3}\sigma^2/\tau_{MD}$ for 50 000 and 90 000 atom structures, respectively. These values are about 10% lower than those obtained from the VAF integrals. This 10% difference is perhaps also related to the partial velocity slip at the fluid-particle interface discussed above (see Fig. 3).

In summary, our analysis of the correlations between a Brownian particle motion and the velocity field in the surrounding fluid demonstrated that the time-integrated response of the fluid has spatial characteristics which are exactly the same as those of a fluid around a particle exhibiting a stationary motion. This result relates to the problem of the diffusion coefficient of a Brownian particle that also characterizes a time-integrated motion and is correctly evaluated with a viscous drag coefficient calculated as if the particle velocity is a constant. Our results demonstrate an origin of the validity of an assumption used in theoretical descriptions of diffusive particles in confined geometries and in colloids, namely that the viscous drag force can be computed as if the particles were moving with constant velocities. It would be highly desirable to have a theoretical justification of Eq. (4),

which at this point is just an empirical observation from our molecular simulation study.

This work was supported by DOE Grant No. DE-FG02-04ER46104. We are grateful for valuable comments provided by Doctor Sanat Kumar (Rensselaer Polytechnic Institute) and Doctor David Cahill (UIUC).

[1] See, for example, L. D. Landau and E. M. Lifshitz, *Fluid Mechanics*, 2nd ed. (Butterworth-Heinemann, Oxford, 1987).
[2] J. Happel and H. Brenner, *Low Reynolds Number Hydrodynamics* (Kluwer, Dordrecht, 1983).
[3] See, for example, M. Takeo, *Disperse Systems* (Wiley-VCH, Weinheim, 1999).
[4] B. Lin, J. Yu, and S. A. Rice, Phys. Rev. E **62**, 3909 (2000).
[5] S. P. Jang and S. U. S. Choi, Appl. Phys. Lett. **84**, 4316 (2004).
[6] R. Prasher *et al.*, Phys. Rev. Lett. **94**, 025901 (2005).
[7] J. Koo and C. Kleinstreuer, J. Nanopart. Res. **6**, 577 (2004).
[8] Y. Pomeau and P. Resibois, Phys. Rep., Phys. Lett. **19**, 63 (1975), and references therein.
[9] G. S. Grest and K. Kremer, J. Chem. Phys. **92**, 5057 (1990), and references therein.
[10] M. P. Allen and D. J. Tildesley, *Computer Simulation of Liquids* (Oxford University Press, Oxford, 1992).
[11] H. Hasimoto, J. Fluid Mech. **5**, 317 (1959).